

# Multi-particle structure in the $\mathbb{Z}_n$ -chiral Potts models

G. von Gehlen\* and A. Honecker\*\*

Physikalisches Institut der Universität Bonn  
Nußallee 12, D 5300 Bonn 1, Germany

**Abstract :** We calculate the lowest translationally invariant levels of the  $\mathbb{Z}_3$ - and  $\mathbb{Z}_4$ -symmetrical chiral Potts quantum chains, using numerical diagonalization of the hamiltonian for  $N \leq 12$  and  $N \leq 10$  sites, respectively, and extrapolating  $N \rightarrow \infty$ . In the high-temperature massive phase we find that the pattern of the low-lying zero momentum levels can be explained assuming the existence of  $n - 1$  particles carrying  $\mathbb{Z}_n$ -charges  $Q = 1, \dots, n - 1$  (mass  $m_Q$ ), and their scattering states. In the superintegrable case the masses of the  $n - 1$  particles become proportional to their respective charges:  $m_Q = Qm_1$ . Exponential convergence in  $N$  is observed for the single particle gaps, while power convergence is seen for the scattering levels. We also verify that qualitatively the same pattern appears for the self-dual and integrable cases. For general  $\mathbb{Z}_n$  we show that the energy-momentum relations of the particles show a parity non-conservation asymmetry which for very high temperatures is exclusive due to the presence of a macroscopic momentum  $P_m = (1 - 2Q/n)/\phi$ , where  $\phi$  is the chiral angle and  $Q$  is the  $\mathbb{Z}_n$ -charge of the respective particle.

published in: J. Phys. A: Math. Gen. **26** (1993) 1275-1298

BONN-HE-92-32  
hep-th/9210125

October 1992

\* e-mail-address: unp02f@ibm.rhrz.uni-bonn.de

\*\* e-mail-address: unp06b@ibm.rhrz.uni-bonn.de

# 1 Introduction

The  $\mathbb{Z}_3$ -chiral Potts model has been introduced in 1981 by Ostlund and Huse in order to describe incommensurate phases of physisorbed systems [1, 2], e.g. monolayer krypton on a graphite surface [3]. The phase structure of several versions of the model has been studied by various methods: Mean field, Monte-Carlo, renormalization group, transfer-matrix partial diagonalization and finite-size scaling of quantum chains [4, 5, 6, 7]. In the following we shall focus mostly on the quantum chain version of the model.

In 1981-82 quantum chain hamiltonians for the chiral Potts model were obtained [8, 9] via the  $\tau$ -continuum limit [10, 11] from the Ostlund-Huse two-dimensional model. These were not self-dual, so that the location of the critical manifold was possible only by finite-size scaling [6, 12]. In 1983 Howes, Kadanoff and DenNijs [13] introduced a self-dual  $\mathbb{Z}_3$ -symmetrical chiral quantum chain, which, however, does not correspond to a two-dimensional model with positive Boltzmann weights. Therefore in the self-dual model the immediate connection to realistic physisorbed systems is lost, but its peculiar mathematical structure has attracted much interest: Howes *et al.* found that the lowest gap of the self-dual model is linear in the inverse temperature, and subsequently in ref. [14] it was shown that the model fulfils the Dolan-Grady integrability conditions [15]. (now usually called "superintegrability" [16]). A whole series of  $\mathbb{Z}_n$ -symmetrical quantum chains has been defined, which satisfy the superintegrability conditions [14]. The Dolan-Grady integrability conditions have been shown to be equivalent to the Onsager algebra [17, 18, 19], which entails that all eigenvalues of the hamiltonian have a simple Ising-type form. The well-known Ising quantum chain in a transverse field is the  $\mathbb{Z}_2$ -version of the superintegrable chiral Potts models.

Much work has been done in the past few years in order to obtain analytic expressions for the complete spectrum of the  $\mathbb{Z}_3$ -superintegrable model [16, 20]. In the next Section we shall quote some of these results. The aim of the present paper is not to add to the analytic calculations of the special superintegrable case, but rather to use numerical finite-size analysis in order to investigate, how the integrable model is embedded in the more general versions of the chiral  $\mathbb{Z}_3$ - and  $\mathbb{Z}_4$ -models. We shall study the low-lying levels of the excitation spectrum and investigate the possibility of a particle interpretation.

In the neighbourhood of conformal points of isotropic theories, very simple particle patterns have been found by Zamolodchikov's perturbation expansion [21], which is applicable to the non-chiral limit of the chiral Potts-models. We shall follow these particle patterns by varying the chiral angles, and try to find out which special properties of the spectrum lead, for particular parameter values, to superintegrability. Since for this purpose we have to study the spectrum through a large probably non-integrable parameter range, at present there is no alternative to numerical methods. It turns out that even in those cases which can be solved analytically, some basic features can be discovered rather easily through a numerical calculation, because the exact formulae are quite involved.

The plan of this paper is as follows: In Sec.2 we start with the basic definitions of the chiral Potts model for general  $\mathbb{Z}_n$ -symmetry, which then are specialized to the  $\mathbb{Z}_3$ - and  $\mathbb{Z}_4$ -cases. Sec.3 collects some basic analytic results which are available for the generic  $\mathbb{Z}_n$ -symmetric model. In Sec.4 we give our detailed finite-size numerical results which confirm the two-particle interpretation of the low-lying spectrum of the self-dual version of the  $\mathbb{Z}_3$ -model. Sec.5 discusses the analogous results for the self-dual version of the  $\mathbb{Z}_4$ -model and shows that the low-lying spectrum is well described in terms of three elementary particles. While up to this point, we consider translationally invariant states only, in Sec.6

we present observations on the energy-momentum dispersion relations of the elementary particles and the effects of parity-violation on the spectrum. Finally, Sec.7 collects our conclusions.

## 2 The chiral $\mathbb{Z}_n$ -Potts quantum chain

The chiral  $\mathbb{Z}_n$ -symmetric Potts spin quantum chain [14] with  $N$  sites is defined by the hamiltonian

$$H^{(n)} = - \sum_{j=1}^N \sum_{k=1}^{n-1} \left\{ \bar{\alpha}_k \sigma_j^k + \lambda \alpha_k \Gamma_j^k \Gamma_{j+1}^{n-k} \right\}. \quad (1)$$

Here  $\sigma_j$  and  $\Gamma_j$  are  $n \times n$ -matrices acting at site  $j$ , which satisfy the relations

$$\sigma_j \Gamma_{j'} = \Gamma_{j'} \sigma_j \omega^{\delta_{j,j'}}, \quad \sigma_j^n = \Gamma_j^n = \mathbf{1}, \quad \omega = \exp(2\pi i/n). \quad (2)$$

A convenient representation for  $\sigma$  and  $\Gamma$  in terms of diagonal and lowering matrices, respectively, is given by

$$(\sigma)_{l,m} = \delta_{l,m} \omega^{l-1}, \quad (\Gamma)_{l,m} = \delta_{l+1,m} \pmod{n}. \quad (3)$$

We shall assume periodic boundary conditions:  $\Gamma_{N+1} = \Gamma_1$ .

The model contains  $2n-1$  parameters: the real inverse temperature  $\lambda$  and the complex constants  $\alpha_k$  and  $\bar{\alpha}_k$ . We shall only consider the case of  $H^{(n)}$  being hermitian:  $\alpha_k = \alpha_{n-k}^*$  and  $\bar{\alpha}_k = \bar{\alpha}_{n-k}^*$ . For  $n > 2$  and generic complex  $\alpha_k$  and  $\bar{\alpha}_k$ , the Perron-Frobenius theorem does not apply and the spectrum of  $H^{(n)}$  may show ground-state level crossings.  $H^{(n)}$  commutes with the  $\mathbb{Z}_n$  charge operator  $\tilde{Q} = \prod_{j=1}^N \sigma_j$ . The eigenvalues of  $\tilde{Q}$  have the form  $\exp(2\pi i Q/n)$  with  $Q$  integer. We shall refer to the  $n$  charge sectors of the spectrum of  $H^{(n)}$  by  $Q = 0, \dots, n-1$ , respectively. Parity is not a good quantum number, but  $H^{(n)}$  is translational invariant, so that each eigenstate of  $H^{(n)}$  can be labelled by its momentum eigenvalue  $p$ .

For  $\alpha_k = \bar{\alpha}_k$  the model is self-dual with respect to the reflection  $\lambda \rightarrow \lambda^{-1}$ . If we choose [14]

$$\alpha_k = \bar{\alpha}_k = 1 - i \cot(\pi k/n) \quad (4)$$

then the model is "superintegrable" [22], i.e. it fulfils the Dolan-Grady [15] conditions and therefore the  $\lambda$ -dependence of all eigenvalues  $E(\lambda)$  of  $H^{(n)}$  has the special Ising-like form [18, 22]:

$$E(\lambda) = a + b\lambda + \sum_j 4m_j \sqrt{1 + 2\lambda \cos \theta_j + \lambda^2}. \quad (5)$$

Here  $a, b$  and  $\theta_j$  are real numbers. The  $m_j$  take the values  $m_j = -s_j, -s_j + 1, \dots, s_j$ , where  $s_j$  is a finite integer. For details concerning formula (5), see [18, 22].

Albertini *et al.* [22, 23] have obtained a spin chain of the form (1) with

$$\alpha_k = e^{i(2k/n-1)\phi} / \sin(\pi k/n), \quad \bar{\alpha}_k = e^{i(2k/n-1)\varphi} / \sin(\pi k/n) \quad (6)$$

$$\cos \varphi = \lambda \cos \phi \quad (7)$$

as a limiting case of an integrable two-dimensional lattice model. The Boltzmann weights of their two-dimensional model do not have the usual difference property [23] and satisfy a new type of Yang-Baxter equations which involve spectral parameters defined on Riemann

surfaces of higher genus. So a quantum chain (1) with coefficients (6), (7) is integrable. The superintegrable case is contained in (6) for  $\varphi = \phi = \pi/2$ .

A number of analytic results is available for the superintegrable case. Some of these will be reviewed in the next Section. Starting 1987, the Stony-Brook-group has published a series of papers [16, 22, 23] which give analytic calculations of the spectrum of the  $\mathbb{Z}_3$ -superintegrable quantum chain. Recently, the completeness of the analytic expressions for the levels of the superintegrable  $\mathbb{Z}_3$ -model has been shown by Dasmahapatra *et al.* [24].

In the non-chiral limiting case  $\varphi = \phi = 0$  of the hamiltonian (1) with coefficients (6) we obtain the lattice version of the parafermionic  $\mathbb{Z}_n$ -symmetrical Fateev-Zamolodchikov-models  $\mathcal{WA}_{n-1}$  [25]. These quantum chains are self-dual. At the self-dual point  $\lambda = 1$  and for  $N \rightarrow \infty$  they show an extended conformal symmetry with central charge  $c = 2(n-1)/(n+2)$ . Exact solutions of these  $\mathcal{WA}_{n-1}$ -hamiltonian chains [26, 27, 28, 29] have been obtained through Bethe-ansatz techniques [28, 30]. Very recently, Cardy [31] has shown that a particular integrable perturbation of the critical  $\mathcal{WA}_{n-1}$ -models leads to self-dual chiral Potts models.

Since later we shall mostly study the  $\mathbb{Z}_3$ - and  $\mathbb{Z}_4$ -versions of (1), we now list how  $H^{(n)}$  specializes for these cases. If we keep insisting on hermiticity,  $H^{(3)}$  depends on three parameters apart from a normalization [13]. In accordance with (6) we write:

$$H^{(3)} = -\frac{2}{\sqrt{3}} \sum_{j=1}^N \left\{ e^{-i\varphi/3} \sigma_j + e^{+i\varphi/3} \sigma_j^\dagger + \lambda \left( e^{-i\phi/3} \Gamma_j \Gamma_{j+1}^+ + e^{+i\phi/3} \Gamma_j^+ \Gamma_{j+1} \right) \right\}. \quad (8)$$

Here  $\sigma_j$  and  $\Gamma_j$  are  $3 \times 3$ -matrices acting at site  $j$ :

$$\sigma_j = \begin{pmatrix} 1 & 0 & 0 \\ 0 & \omega & 0 \\ 0 & 0 & \omega^2 \end{pmatrix}_j, \quad \Gamma_j = \begin{pmatrix} 0 & 0 & 1 \\ 1 & 0 & 0 \\ 0 & 1 & 0 \end{pmatrix}_j \quad (9)$$

and  $\omega = \exp(2\pi i/3)$ . We shall consider  $0 \leq \lambda \leq \infty$ ;  $0 \leq \phi, \varphi \leq \pi$  (for reflection properties of  $H^{(3)}$  see [13]). In order not to get lost in three-dimensional diagrams, often we shall concentrate on two cases in which there is one relation between the three parameters: the integrable case (INT), where the three parameters are related by eq.(7), and the self-dual case (SD) where  $\phi = \varphi$ . For generic  $\varphi$  and  $\lambda$ , the self-dual case is not known to be integrable. The SD case contains the non-chiral limit  $\varphi = \phi = 0$ , in which we obtain the  $\mathcal{WA}_2$ -model, which coincides with the  $\mathbb{Z}_3$ -standard Potts model. It has a second-order phase transition at  $\lambda = 1$ , which for  $N \rightarrow \infty$  is described by a conformal field theory with central charge  $c = 4/5$  [32, 33, 34].

The phase diagram of the SD-chiral  $\mathbb{Z}_3$ -model shows four different phases [22, 35, 36], see Fig. 1: for small chiral angle  $\varphi$  we have oscillating massive high- and low-temperature phases at  $\lambda < 1$  and  $\lambda > 1$ , respectively, except for a small incommensurate phase interval around  $\lambda = 1$ . The two incommensurate phases appear centered around  $\lambda = 1$  and get wider in  $\lambda$  as  $\varphi$  increases.

The hermitian  $\mathbb{Z}_4$ -symmetric  $H^{(4)}$  contains five parameters (again apart from a normalization), which we denote by  $\lambda, \phi, \varphi, \beta$  and  $\tilde{\beta}$ :

$$H^{(4)} = -\sqrt{2} \sum_{j=1}^N \left\{ e^{-i\varphi/2} \sigma_j + \beta \sigma_j^2 + e^{i\varphi/2} \sigma_j^3 + \lambda \left[ e^{-i\phi/2} \Gamma_j \Gamma_{j+1}^3 + \tilde{\beta} \Gamma_j^2 \Gamma_{j+1}^2 + e^{i\phi/2} \Gamma_j^3 \Gamma_{j+1} \right] \right\} \quad (10)$$

where  $\sigma_j$  and  $\Gamma_j$  are now  $4 \times 4$ -matrices obeying (3). For simplicity, and in agreement with (6), we shall consider only the case  $\beta = \tilde{\beta} = 1/\sqrt{2}$ , so that we have again two parameters for the non-self-dual integrable version, and two parameters  $\lambda$  and  $\phi = \varphi$  for the self-dual case. For  $\varphi = \phi = 0$  and  $\beta = \tilde{\beta} = 1/\sqrt{2}$  the hamiltonian (10) coincides with that of the Ashkin-Teller quantum chain [37] for the special value  $h = 1/3$  in the notations of [38]. From the phase diagram of the Ashkin-Teller quantum chain we know that in the case  $h = 1/3$  there is just one critical point at the self-dual value  $\lambda = 1$ . This is described by the  $\mathcal{WA}_3$  rational model at  $c = 1$ , which has an extended conformal symmetry with fields of spin three and four.

### 3 General results for the energy gaps of the $\mathbb{Z}_n$ -chiral Potts model

Apart from the exact results for the non-chiral limiting case just mentioned at the end of the last section, there are many exact results for the superintegrable case (1), (4) (equivalent to (6) with  $\varphi = \phi = \pi/2$ ): The  $\mathbb{Z}_2$ -case, which is the standard Ising quantum chain in a transverse field, has been solved in refs. [10, 11, 39]. Recently, as mentioned above, also the complete spectrum of the  $\mathbb{Z}_3$ -superintegrable quantum chain has been calculated analytically [24]. We shall first collect some important partial results which are available for *generic*  $\mathbb{Z}_n$ .

In order to state these, we shall define all gaps with respect to the lowest  $Q=0, p=0$ -level, which we denote by  $E_0(Q=0, p=0)$ . Note that  $E_0(Q=0, p=0)$  is not necessarily the ground state of the hamiltonian. Depending on the parameters chosen, the ground state may be in any charge sector and may even have non-zero momentum  $p$ , since the model contains incommensurate phases. Nevertheless, in this section let us consider only gaps between  $p=0$ -levels.

By  $\Delta E_{Q,i}$  we denote the energy difference

$$\Delta E_{Q,i} = E_i(Q, p=0) - E_0(Q=0, p=0) \quad (11)$$

where  $E_i(Q, p=0)$  is the  $i$ -th level ( $i = 0, 1, \dots$ ) of the charge  $Q$ , momentum  $p=0$ -sector. In the  $\mathbb{Z}_2$ -(Ising)-case of (1) it is well-known that the lowest gap  $\Delta E_{1,0}$  has the remarkable property of being linear in  $\lambda$ :

$$\Delta E_{1,0} = 2(1 - \lambda). \quad (12)$$

In 1983 Howes, Kadanoff and DenNijs [13] found that the same is true also for the self-dual version of the  $\mathbb{Z}_3$ -chiral Potts model, eq.(8) at the special chiral angle  $\varphi = \phi = \pi/2$ . They discovered this by calculating the high-temperature expansion up to 10th order in  $\lambda$ , finding that for these special angles all higher coefficients in the expansion, starting with the coefficient of  $\lambda^2$ , are zero.

In [14] it was the desire to generalize (12) so as to obtain for *all*  $\mathbb{Z}_n$  and *all*  $Q$  the simple formula

$$\Delta E_{Q,0} = 2Q(1 - \lambda) \quad (\lambda < 1, \quad Q = 1, \dots, n-1) \quad (13)$$

which lead to choose the values (4) for the coefficients  $\alpha_k$  and  $\bar{\alpha}_k$  and to find the superintegrability of the model. In [14] the linearity of the gaps was checked through numerical calculations. The validity of (12) for the superintegrable  $\mathbb{Z}_3$ -model to all orders of a perturbation expansion in  $\lambda$  was first shown in [23] using a recurrence formula. Later, using

analytic methods, Albertini *et al.* [22, 23] for the superintegrable  $\mathbb{Z}_3$ -case, and then Baxter [20] for all superintegrable  $\mathbb{Z}_n$ , have calculated the lowest gaps of the hamiltonian eq.(1) in the thermodynamic limit  $N \rightarrow \infty$ .

Using the definition (11), Baxter's analytic results for the superintegrable model can be summarized in the form:

$$\Delta E_{Q=1,0} = 2(1 - \lambda) \quad (\lambda < 1) \quad (14)$$

$$\Delta E_{Q=0,1} = 2n(\lambda - 1) \quad (\lambda > 1) . \quad (15)$$

We now attempt to interpret the spectrum of (1) and the gap formula (13) in terms of particle excitations. Consider first eq.(13). This would be obtained if the model contained only one single particle species with mass  $m_1 = 2(1 - \lambda)$  and  $\mathbb{Z}_n$ -charge  $Q = 1$ . The lowest  $\Delta Q \neq 1$ -gaps would then arise from the thresholds of the scattering of  $Q$  of these  $Q=1$ -particles.

In order to check whether it is correct to describe the spectrum at  $\varphi = \phi = \pi/2$  this way, or whether more fundamental particles must be present, we shall study the zero momentum part of the spectrum as a function of the chiral angles, when these move away from the special superintegrable values. We shall start considering the spectrum down at  $\varphi = \phi = 0$ , where we know the particle structure from the thermally perturbed  $\mathcal{WA}_{n-1}$ -models and move then towards higher chiral angles.

The scaling regime around  $\lambda = 1$  of the  $\mathcal{WA}_{n-1}$ -models is known to contain  $n - 1$  particle species, one in each of the non-zero  $\mathbb{Z}_n$ -charge sectors  $Q = 1, \dots, n - 1$ . The ratios of their masses  $m_Q$  are [40]:

$$\frac{m_Q}{m_1} = \frac{\sin(\pi Q/n)}{\sin(\pi/n)}, \quad (Q = 1, \dots, n - 1). \quad (16)$$

The particles with masses  $m_Q$  and  $m_{n-Q}$  form particle-antiparticle-pairs. Near  $\lambda = 1$  the mass scale  $m_1$  behaves as

$$m_1 \sim (1 - \lambda)^{(n+2)/2n}. \quad (17)$$

as it follows from the conformal dimension  $x = 4/(n + 2)$  of the leading thermal operator of the  $\mathcal{WA}_{n-1}$ -model. Looking at (16), we can see that in the scaling  $\mathcal{WA}_{n-1}$ -model all particles are *isolated* non-degenerate levels in the spectrum of their respective charge sector. E.g. for the particle with mass  $m_Q$  to be on the scattering threshold of  $Q$  of the lightest particles with mass  $m_1$ , we must have  $Q \sin(\pi/n) = \sin(Q\pi/n)$ , which is possible only in the limit  $n \rightarrow \infty$ . Similarly, e.g. for  $n \geq 5$ , the  $m_4$ -particle is below the threshold  $m_2 + m_2$ , and approaches this threshold only as  $n \rightarrow \infty$ .

We now want to follow these single particle levels in  $\lambda$  to outside the scaling region and as functions of the chiral angles  $\varphi$  and  $\phi$ , in order to get information about what will happen at  $\varphi, \phi \rightarrow \frac{\pi}{2}$ . Since near  $\lambda = 1$  the gaps can only be calculated numerically for generic  $\phi, \varphi$  (we shall report such numerical calculations later), it is most simple to consider first the small- $\lambda$ -expansion for the lowest  $p = 0$ -gaps of the hamiltonian (1). Using the coefficients in the form (6), but not assuming (7), to first order in  $\lambda$  we get:

$$\begin{aligned} \Delta E_{Q,0} &= \left( \sum_{k=1}^{n-1} \bar{\alpha}_k (1 - \omega^{Qk}) \right) - \lambda(\alpha_Q + \alpha_{n-Q}) + \dots \\ &= \left( \sum_{k=1}^{n-1} \frac{2 \sin(\pi k Q/n)}{\sin(\pi k/n)} \sin \left( \left( \frac{2k}{n} - 1 \right) \varphi + \frac{\pi k Q}{n} \right) \right) - \frac{2\lambda}{\sin(\pi Q/n)} \cos \left( \left( \frac{2Q}{n} - 1 \right) \phi \right) + \dots \end{aligned} \quad (18)$$

Eq.(18) fulfils the CP-relation

$$\Delta E_{Q,i}(\lambda, \varphi, \phi) = \Delta E_{n-Q,i}(\lambda, -\varphi, -\phi) \quad (i = 0, 1, \dots) \quad (19)$$

In the sum in (18), the pairs of terms for  $k$  and  $n - k$  are equal.

For  $\varphi = 0$  and for  $\varphi = \frac{\pi}{2}$  it is easy to simplify eq.(18) using the trigonometrical sum formulae [41, 42]

$$\begin{aligned} \sum_{k=1}^{n-1} \sin(k\pi/n) &= \cot \frac{\pi}{2n}, & \sum_{k=1}^{n-1} \sin^2(k\pi Q/n) &= n/2, \\ \sum_{k=1}^{n-1} \sin^3(k\pi/n) &= \frac{1}{4} \left( 3 \cot \frac{\pi}{2n} - \cot \frac{3\pi}{2n} \right) && \text{etc.} \end{aligned} \quad (20)$$

For  $\varphi = \phi = 0$  we obtain:

$$\Delta E_{1,0} = 2 \cot \frac{\pi}{2n} - \frac{2\lambda}{\sin(\pi/n)} + \dots \quad (21)$$

and

$$\Delta E_{2,0} = 2 \cot \frac{\pi}{2n} + 2 \cot \frac{3\pi}{2n} - \frac{2\lambda}{\sin(2\pi/n)} + \dots \quad (22)$$

We identify

$$m_Q \equiv \Delta E_{Q,0}, \quad (23)$$

and conclude from (16) and (22) that the mass ratio  $m_2/m_1$  must decrease when going from the scaling region  $\lambda \approx 1$  to  $\lambda = 0$ . E.g. for  $n = 4$ , eq.(16) gives  $m_2/m_1 = \sqrt{2}$ , whereas at  $\lambda = 1$  from (21) and (22) we get  $m_2/m_1 \approx 1.17157$ . Observe, that also according (22),  $m_2$  stays below the  $Q = 2$ -sector threshold at  $2m_1$ , and generally, the lowest levels of each charge sector remain isolated down to  $\lambda = 0$ .

We now look how the perturbation formula (18) behaves in the superintegrable limit. Inserting  $\varphi = \phi = \pi/2$ , we obtain

$$\Delta E_{Q,0} = 2 \sum_{k=1}^{n-1} \sin^2(\pi k Q/n) - \sum_{k=1}^{n-1} \sin(2\pi k Q/n) \cot(\pi k/n) - 2\lambda + \dots \quad (24)$$

The sums can be calculated explicitly, leading to the simple result

$$\Delta E_{Q,0} = 2(Q - \lambda) + O(\lambda^2). \quad (25)$$

Comparing (25) to (13), we have an apparent contradiction, since in (25) the factor  $Q$  is *not* multiplying  $\lambda$ .

Our detailed non-perturbative numerical analysis of the spectrum for the  $\mathbb{Z}_3$ - and  $\mathbb{Z}_4$ -cases (to be discussed in the next Section) shows that the single particle levels vary smoothly when increasing  $\varphi$  and  $\phi$  starting from  $\varphi = \phi = 0$ . As soon as the chiral angles become non-zero, the particle-antiparticle-pairs  $m_Q$  and  $m_{n-Q}$  split:  $m_1$  decreases and  $m_{n-1}$  increases as  $\varphi, \phi$  increase. Approaching  $\varphi = \phi = \pi/2$ ,  $m_2$  becomes twice as large as  $m_1$ , so that at  $\varphi = \phi = \pi/2$ ,  $m_2$  sits just at the  $m_1 + m_1$ -scattering threshold. So, our non-degenerate perturbation theory should break down for the channel  $Q = 2$  at  $\varphi, \phi \geq \frac{\pi}{2}$  [13], and, indeed we see this in the calculation of the  $\lambda^2$ -contribution to  $\Delta E_{2,0}$ . Because

for general  $\mathbb{Z}_n$  the explicit expression for the  $\lambda^2$ -term in (18) is too involved, here we specialize and give the result for the self-dual  $\mathbb{Z}_3$ -case. We find

$$\Delta E_{1,0}(\varphi, \lambda) = 4 \sin \frac{\pi - \varphi}{3} - \frac{4\lambda}{\sqrt{3}} \cos \frac{\varphi}{3} + \lambda^2 f(\varphi) + O(\lambda^3). \quad (26)$$

where

$$f(\varphi) = -\frac{1}{3 \cos \varphi} \left( 2 \sin \frac{\pi - 4\varphi}{3} - 4 \sin \frac{\pi + 2\varphi}{3} + 3\sqrt{3} \right). \quad (27)$$

$f(\varphi)$  is smooth at  $\varphi = \frac{\pi}{2}$  (we have  $f(\frac{\pi}{2}) = -\sqrt{3}/2$ ), but it is singular for  $\varphi \rightarrow -\frac{\pi}{2}$ . Applying (19), from (26) we get  $\Delta E_{2,0}$ :

$$\Delta E_{2,0}(\varphi, \lambda) = 4 \sin \frac{\pi + \varphi}{3} - \frac{4\lambda}{\sqrt{3}} \cos \frac{\varphi}{3} + \lambda^2 f(-\varphi) + O(\lambda^3). \quad (28)$$

While formula (26) for  $\Delta E_{1,0}$  can be used in the whole range  $0 \leq \varphi < \pi$  (considering non-negative  $\varphi$ ), the corresponding expression (28) is valid only for  $0 \leq \varphi < \frac{\pi}{2}$  and diverges at  $\varphi = \phi = \frac{\pi}{2}$ . The  $\lambda^2$ -contribution to the analogous  $\mathbb{Z}_4$ -formula will be given in Sec.5. It shows a similar divergence in the expression for  $m_2$ .

Since (28) breaks down at  $\varphi = \pi/2$ , we need further information in order to decide whether the  $Q = 2$ -particle survives at and beyond  $\varphi = \pi/2$ . Then this will clarify the question whether the single particle picture described above makes sense at the superintegrable line.

## 4 Finite-size numerical calculation of the low-lying spectrum of the $\mathbb{Z}_3$ -chiral quantum chain

### 4.1 Convergence exponent $y$

We shall now describe several detailed numerical checks of the two-particle picture from the spectrum in the high-temperature massive region of the  $\mathbb{Z}_3$ -model. For this purpose, we have calculated numerically the eight lowest  $p = 0$ -levels of each charge sector of the hamiltonian (8) for  $N = 2, \dots, 12$  sites. While in the last Section, we concentrated on the single particle levels, now we shall also look into the scattering states and check, whether the corresponding thresholds appear as expected.

For chains of up to  $N = 8$  sites we are able to diagonalize  $H^{(3)}$  exactly. Using Lanczos diagonalization we can use up to  $N = 12$  sites. We shall always give the results for periodic boundary conditions, but we have also partially checked the results with twisted boundary conditions. The extrapolation to  $N \rightarrow \infty$  is done using both the Van-den-Broeck-Schwartz algorithm [43] and rational approximants [44] (for details on the application to quantum chains and error estimation see [45]).

Neighbouring higher levels sometimes cross over as functions of the number of sites  $N$ , so that for these there is a danger of connecting wrong sequences. This can be controlled by calculating the leading power of the convergence,  $y$ , defined by

$$\Delta E(N) - \Delta E(\infty) = N^{-y} + \dots \quad (29)$$

and checking the smoothness of the approximants  $y_N$ :

$$y_N = -\ln\left(\frac{\Delta E(N) - \Delta E(\infty)}{\Delta E(N-1) - \Delta E(\infty)}\right) / \ln\left(\frac{N}{N-1}\right) \quad (30)$$

In (29) and (30),  $\Delta E(N)$  is a gap  $\Delta E_{Q,i}$  calculated for  $N$  sites.

The calculation of  $y_N$  is also very useful for distinguishing between single particle levels and two- or more particle scattering states: For single particle levels we expect

$$\Delta E(N) - \Delta E(\infty) = \exp(-N/\xi) + \dots \quad (31)$$

i.e. exponential convergence in  $N$  ( $\xi$  is a correlation length), so that for these the  $y_N$  should increase very fast with  $N$ . In contrast to this, for two-particle states we should have a power behaviour in  $N$ , more precisely, we should have  $\lim_{N \rightarrow \infty} y_N = 2$ .

## 4.2 The spectrum for the superintegrable case $\varphi = \pi/2$

We first discuss our numerical results for the  $\mathbb{Z}_3$ -superintegrable case  $\phi = \varphi = \pi/2$ . Table 1 lists results for 16 low-lying gaps for  $\lambda = 0.5$  in the high-temperature regime, where from (12) we know that  $m_1 \equiv \Delta E_{Q=1,0} = 1$ . As we have checked by repeating the calculation for several other values of  $\lambda < 1$ , this value  $\lambda = 0.5$  is not special regarding the structure of the spectrum. However, there is the nice feature that because of (13) for this  $\lambda$  the gaps should approach integer values in the limit  $N \rightarrow \infty$ .

In the  $Q = 1$ -sector we see an isolated lowest state at  $m_1 = 2(1 - \lambda)$  followed by a bunch of levels at  $4m_1$ . Looking into Table 2 which gives the convergence with  $N$  as parametrized by  $y$  according to (29), we see that indeed the  $m_1$ -level ( $Q=1$ ; column  $i = 0$ ) shows exponential convergence, whereas the levels  $Q = 1$ ;  $i = 1, 2$  converge as  $N^{-3}$  and  $N^{-2}$ , respectively. This indicates that the  $i = 1$ -level is due to 3-particle ( $m_1 + m_1 + m_1$ )-scattering, and the  $i = 2$ -level due to 2-particle ( $m_2 + m_2$ )-scattering as written in the bottom line in Table 1.

The  $Q = 2$ -sector shows no isolated ground state, but starts with a bunch of levels around  $\Delta E = 2$ . There is strong evidence for another bunch around  $\Delta E = 5$ , of which Table 1 shows just the first level. The convergence for the further  $\Delta E = 5$ -levels is poor and we do not give the numbers. A clue to the nature of the  $\Delta E = 2$ -levels is found through their convergence for increasing  $N$ : Table 2 shows clearly that the level labelled  $Q=2$ ;  $i=0$  has an  $N$ -dependence which drastically differs from that of the other levels, indicating that this is the level of a single particle with mass  $m_2 = 4(1 - \lambda)$  (we have checked the  $\lambda$ -dependence repeating the calculation for six other values of  $\lambda$ ). So, we can answer the question posed at the end of the last Section: The  $m_2$ -level can be clearly seen in the superintegrable case, although it lies at the edge of the scattering threshold. The power-behaved  $Q = 2$ -states at  $\Delta E = 2$  should then be interpreted as  $m_1 + m_1$ -states. The level  $Q = 2$ ;  $i = 5$  may be  $m_1 + m_2 + m_2$ , which has the correct total  $\mathbb{Z}_3$ -charge  $Q = 2$ .

The pattern at  $Q = 0$ ,  $\Delta E = 3$  is as expected by this picture: There should be  $m_1 + m_2$ -states and  $m_1 + m_1 + m_1$ -states, both distinguished by different values of  $y$ , as observed in Tables 1 and 2.

For other values of  $\lambda$  ranging from  $\lambda = 0.2$  to  $\lambda = 0.8$  we find precisely the same structure. Not surprisingly, above  $\lambda = 0.8$  the convergence with respect to  $N$  is getting poor, since the relevant mass scale  $m_1$  is vanishing as  $\lambda \rightarrow 1$  and so at  $\lambda = 0.8$  it is already quite small.

## 4.3 The spectrum off the superintegrable line

After having found a simple two-particle pattern in the superintegrable case, we now check how this structure gets modified for  $\varphi, \phi \neq \frac{\pi}{2}$ . In order not to vary too many parameters,

we consider only the INT and SD cases defined at the end of Sec.2. For the INT-case explicit formulae for the spectrum are not yet available (for some first attempts, see [46]). For the SD-case there may be no integrability at all. So, for the following, presently there is no alternative to our numerical or perturbative methods.

We start with the SD case. In Sec.3 we discussed already the perturbation expansion of the lowest gaps to order  $\lambda^2$ . This indicated that, increasing  $\varphi$  from the Potts-value  $\varphi = 0$  to  $\varphi = \pi/2$  for fixed  $\lambda < 1$  the mass  $m_1$  decreases and  $m_2$  increases until for  $\varphi = \pi/2$  we reach the value  $m_2/m_1 = 2$ . Above  $\varphi = \pi/2$  we then should have  $m_2/m_1 > 2$  which makes it difficult to isolate the  $Q = 2$ -particle in the  $m_1 + m_1$ -continuum (in case it is still there at all). Fig.2 shows the different patterns which we expect in the three charge sectors for  $\varphi < \pi/2$  (left hand side) and for  $\varphi > \pi/2$  (right). The extrapolation of the finite-size numbers reported in Table 3 confirms all details of these expected patterns. For  $\varphi = 2\pi/3$ , among the three lowest  $Q = 2$  levels at  $\Delta E = 2m_1$  we see no exponentially converging level. For  $\varphi > \pi/2$  all thresholds are determined by  $m_1$  alone, these are  $3m_1$ ,  $4m_1$  and  $2m_1$  for  $Q = 0, 1, 2$ -sectors, respectively.

In order to see, whether the  $Q = 2$ -particle survives in the  $\varphi > \pi/2$ -region, we have to look for more and higher levels. For *small*  $\lambda$  we know from eq.(28) (supposing this to be still valid) where to search for  $m_2$  at  $\varphi > \pi/2$ , and so we have looked slightly above the superintegrable line at  $\varphi = 7\pi/12$ ,  $\lambda \leq 0.25$  among the 8 lowest levels for a fast converging one. Indeed, as it is shown in Table 4, the level  $i = 6$  of the Table converges much faster than its neighbours. So, it is a good candidate for the  $m_2$ -level. However, with increasing  $\lambda$  this convergence diminishes quite fast and an even/odd- $N$  hopping takes over. This may be due to an increasing instability of the  $m_2$ -particle.

For  $\varphi < \pi/2$  the threshold in the  $Q = 0$ -sector depends also on  $m_2$ , being  $m_1 + m_2$ . The left column of Table 3 shows that the numerical values for the various thresholds come out very well and that e.g.  $m_2/m_1 = 1.47755$  at  $\varphi = \pi/4$  and  $\lambda = 0.5$ . Unfortunately, the determination of the corresponding values for  $y$  is quite unsafe, since for  $\varphi \neq \frac{\pi}{2}$  we have no exact values for  $\lim_{N \rightarrow \infty} \Delta E_i$  available as we had in the superintegrable case from (13). So the results we obtain for the  $y_N$  depend strongly on the very unprecise extrapolated results which are used for  $\Delta E_i(\infty)$ .

#### 4.4 The integrable case for $\varphi \neq \pi/2$

Turning now to the integrable case INT, our data in Table 5 show the same pattern as in the SD case, only the convergence is less good (for the sake of brevity we have omitted the finite-size data). It is not clear whether the  $\Delta E_{Q=2,0}$ -level converges exponentially at all. This result is somewhat surprising, because one might have expected a more clear particle behaviour in the integrable case. We recall that nothing is known about the integrability of the general SD case.

There is not much difference between the SD-case Table 3 and the INT-case Table 5. E.g. observe that in the right hand part of Table 5, which gives an example for chiral angles above the superintegrable value, the low-lying gaps come out clearly as integer multiples of the single scale  $m_1$ , as it is expected for threshold values if  $m_2 > 2m_1$ . The numerical precision is not very good because in the neighbourhood of the incommensurate phase the finite-size approximants to e.g.  $m_1$  first fall with  $N$  and then rise again, a property which is not easy to handle by usual extrapolation procedures.

Apart from the just mentioned non-monotonous behaviour of the gaps for increasing  $N$ , the onset of the IC-phase is not felt in our study of the  $p = 0$ -levels even at  $\varphi = \phi = 5\pi/6$ ,

$\lambda = 0.5$ . For still larger angles, it becomes difficult and then practically impossible to arrange the gaps for various  $N$  into plausible sequences. Anyway, it is already surprising that for  $\varphi = \pi/2$  and higher, the low  $p = 0$ -gaps do not seem to take any notice of the incommensurate phase boundary, and vanish smoothly for  $\lambda \rightarrow 1$ .

In the low-temperature regime  $\lambda > 1$  the pattern of the lowest levels is the same in all three charge sectors: As expected, in the limit  $N \rightarrow \infty$  the ground state is three-fold degenerate (one isolated level in each charge sector). Above the ground state we find for  $\varphi < \pi/2$  a gap which is  $\lambda(m_1(\lambda^{-1}) + m_2(\lambda^{-1}))$ . Then we see a quite dense sequence of levels starting after a gap of  $3\lambda m_1(\lambda^{-1})$  (the same gap in all three charge sectors). If we would have normalized  $H^{(3)}$  including a factor  $\sqrt{\lambda}$  in the denominator of (8), the gaps would be just the same as those in the  $Q = 0$  sector at the duality reflected value of  $\lambda$ . This is a generalization of Baxter's result (15) for the superintegrable case to  $\varphi < \frac{\pi}{2}$ .

## 5 Perturbative and finite-size numerical results for the spectrum of the chiral $\mathbb{Z}_4$ -quantum chain

In the last section we have reported our numerical evidence for a two-particle picture of the spectrum of the off-critical chiral  $\mathbb{Z}_3$ -Potts quantum chain. In this Section we shall show analogous numerical evidence for a three-particle structure in the high-temperature regime of the chiral  $\mathbb{Z}_4$ -Potts quantum chain.

We start giving the high-temperature expansion of the lowest gaps of the self-dual  $\mathbb{Z}_4$ -quantum chain up to order  $\lambda^2$ . It reads explicitly:

$$\Delta E_{1,0} = 2(1 + 2 \sin \frac{\pi - 2\varphi}{4}) - 2\lambda\sqrt{2} \cos(\varphi/2) + \lambda^2 g(\varphi) + \dots \quad (32)$$

$$\Delta E_{2,0} = 4\sqrt{2} \cos(\varphi/2) - 2\lambda + \lambda^2 h(\varphi) + \dots \quad (33)$$

$$\Delta E_{3,0} = 2(1 + 2 \sin \frac{\pi + 2\varphi}{4}) - 2\lambda\sqrt{2} \cos(\varphi/2) + \lambda^2 g(-\varphi) + \dots \quad (34)$$

where  $g$  and  $h$  are the following functions:

$$g(\varphi) = \frac{1 + \sqrt{2} \sin(\varphi/2)}{2 \sin((2\varphi + \pi)/4)} + \frac{4 \sin^2 \varphi + 5 \sin \varphi - 8\sqrt{2} \cos(\varphi/2) - 1}{4\sqrt{2} \cos \varphi \cos(\varphi/2)} \quad (35)$$

$$h(\varphi) = -\frac{2}{\cos \varphi} \left( 1 - \sqrt{2} \cos(\varphi/2) + 2 \cos^2(\varphi/2) \right) \quad (36)$$

The function  $h(\varphi)$  is singular for  $\varphi \rightarrow \frac{\pi}{2}$ , similarly,  $g(\varphi)$  is singular for  $\varphi \rightarrow -\frac{\pi}{2}$ . Of course, (34) follows from (32) by a CP-transformation, see (19). At  $\varphi = \phi = 0$  the sectors  $Q = 1$  and  $Q = 3$  are degenerate.

At  $\varphi = 5\pi/6$  and  $\lambda = 0$ , according to (32) the gap  $\Delta E_{1,0}$  vanishes, and above this value of  $\varphi$  the ground state of the system is in the  $Q = 1$ -sector. This feature is due to the particular choice  $\beta = 1/\sqrt{2}$  which we made after (10). If we consider more general  $\beta$ , then this ground-state level crossing moves to  $\varphi = \pi/2 + 2 \sin^{-1}(\beta/\sqrt{2})$ . So, for  $\beta \geq 1$  the ground state remains in the sector  $Q = 0$  up to  $\varphi = \pi$ .

For  $\varphi$  above its superintegrable value  $\varphi = \frac{\pi}{2}$  (with  $\beta = 1/\sqrt{2}$ ) the scattering thresholds in all sectors are determined by  $m_1 \equiv \Delta E_{1,0}$  alone, and the "single-particle gaps" eqs.(33) and (34) move above the scattering thresholds in the sectors  $Q = 2$  and  $Q = 3$ , respectively. This is quite analogous to what happened in the  $Q = 2$ -sector of the  $\mathbb{Z}_3$ -model.

For all  $\lambda > 0$  the  $Q = 2$ -gap is larger than both the  $Q = 1$ - and  $Q = 3$ -gaps. For small values of  $\lambda$  both  $\Delta E_{1,0}$  and  $\Delta E_{2,0}$  decrease with increasing  $\varphi$ , while  $\Delta E_{3,0}$  grows. At  $\varphi = \pi/2$  the gaps are integer-spaced.

The high-temperature-expansion is reliable for small  $\lambda$  and the lowest levels only. So, for larger values of  $\lambda$ , we have calculated the six lowest  $p = 0$ -levels of each charge sector for the hamiltonian (10) numerically. In the  $\mathbb{Z}_4$ -case we are able to handle up to  $N = 10$  sites only. Correspondingly, the extrapolations are less precise than in the case of  $\mathbb{Z}_3$ .

First, we present our results for some low-lying levels in the spectrum for the super-integrable case of (10):  $\varphi = \phi = \pi/2$ ,  $\beta = \tilde{\beta} = 1/\sqrt{2}$ . Table 6 contains the results at  $\lambda = 0.5$ , where from (13) we should have  $m_1 = 1$ , so that we expect the gaps for  $N \rightarrow \infty$  to approach simple integers. Indeed, this comes out well from our numbers. As before, we have checked for four other values of  $\lambda$  that otherwise there is nothing special about choosing  $\lambda = 0.5$ .

In each of the  $Q \neq 0$ -sectors we see one level which shows very fast convergence with  $N$ , and we identify this with the single-particle state of mass  $m_Q = Q$ .

In the charge sector  $Q = 0$  we can evaluate the four lowest gaps precisely enough to assign them to  $\Delta E = 4$ . There should be four different types of scattering states:  $m_1+m_1+m_1+m_1$ ,  $m_1+m_1+m_2$ ,  $m_2+m_2$  and  $m_1+m_3$ . While the exponents determine the first two types, we would have to move away from  $\varphi = \phi = \pi/2$  in order to distinguish the two latter states. In the sector  $Q = 1$  we see two excited states in addition to the  $m_1$ -particle state. They could be one three-particle- and one two-particle scattering-state, both with  $\Delta E = 5$ . This is compatible with the expected states  $m_1+m_2+m_2$  and  $m_2+m_3$ .

The numerical convergence of the scattering levels and the possibility of ordering the levels into clear sequences in  $N$  gets worse if we consider the sectors  $Q = 2$  and  $Q = 3$ . In the bottom line of Table 6 we give a few quite safe assignments.

We now look numerically, how this particle pattern gets modified if we choose values of the parameters  $\phi \neq \pi/2$ ,  $\varphi \neq \pi/2$  for which no analytic results are available. In Table 7 we have collected the first few lowest energy gaps for three choices of the parameters.

First, we look at values of  $\phi = \varphi < \pi/2$ . For  $\phi = \varphi = \pi/4$  (which is half-way to the  $\mathcal{W}$ -point) and  $\lambda = 0.5$  the masses of the  $m_2$ - and  $m_3$ -states are clearly below the scattering thresholds and the remaining levels can excellently be explained as multi-particle states. In the charge-sector  $Q = 2$  there is one state with  $\Delta E = 4.6$  which seems to be unexplained by this pattern. However, the extrapolation  $N \rightarrow \infty$  is quite delicate and therefore the errors may be too small. Thus, this state could also be a  $2m_1$ -state.

If we choose  $\phi = \varphi > \pi/2$ , the low-lying levels of the spectrum are given by  $m_1$  alone. However, for small values of  $\lambda$  and  $\phi$  slightly above the super-integrable line the  $Q = 2$ -charge-sector shows a high level that converges very fast and is not an integral multiple of  $m_1$ . The middle part of table 7 contains the explicit values for  $\phi = \varphi = 3\pi/5$  and  $\lambda = 0.10$ . Here, the  $m_2$ -particle is still clearly visible as a high level in the  $Q = 2$  sector. Unfortunately, the  $m_3$ -particle is not visible in the  $3m_1$ -continuum.

The right column of Table 7 shows that basically the same patterns can also be observed in the INT case although here the approximation is less good.

To summarize, our numerical data supports a three-particle interpretation of the low-lying spectrum for the chiral  $\mathbb{Z}_4$ -Potts quantum chain with  $\varphi$  in the range from 0 to slightly above  $\pi/2$ .

## 6 Energy momentum relations for the single particle states

When interpreting the excitations of the model in terms of particles, we should also look for their energy-momentum dispersion rule. On a lattice with  $N$  sites and periodic boundary conditions, the momentum  $p$  can take the  $N$  values

$$p = -[\frac{N}{2}], \dots, -1, 0, 1, \dots, [\frac{N}{2}]. \quad (37)$$

In calculating the limit  $N \rightarrow \infty$  we use

$$P = \frac{2\pi}{N} p \quad (-\pi \leq P \leq \pi) \quad (38)$$

Except for the  $\mathcal{WA}_{n-1}$ -case  $\phi = \varphi = 0$  the hamiltonian (1) does not conserve parity, so, in general the curves  $E(P)$  will not be symmetrical with respect to  $P \rightarrow -P$ .

An expansion to first order in  $\lambda$  gives a first orientation of the energy-momentum relation near  $\lambda = 0$  for generic  $\mathbf{Z}_n$ . In an easy generalization of (18) we find for  $Q \neq 0$ :

$$\begin{aligned} \Delta E_{Q,0} &= \left( \sum_{k=1}^{n-1} \bar{\alpha}_k (1 - \omega^{Qk}) \right) - \lambda (e^{iP} \alpha_Q + e^{-iP} \alpha_{n-Q}) + \dots \\ &= \left( \sum_{k=1}^{n-1} \bar{\alpha}_k (1 - \omega^{Qk}) \right) - \frac{2\lambda}{\sin(\pi Q/n)} \cos(P - P_m) + \dots, \end{aligned} \quad (39)$$

where

$$P_m = (1 - 2Q/n)\phi. \quad (40)$$

In the second line of (39) we have inserted the definition (6) of  $\alpha_k$  in the  $\lambda$ -dependent term. Since, to first order in  $\lambda$ , the first term of (39) contains no  $P$ -dependence, we see that in the high-temperature limit, the violation of parity in the dispersion relation of the particle with charge  $Q$  is exclusively due to the presence of a macroscopic momentum  $P_m$  as given in (40). A particle and its antiparticle feel macroscopic momenta which are opposite in sign.

In the parity conserving case  $\varphi = \phi = 0$  the system can be made isotropic between space and euclidian time rescaling the hamiltonian by a suitable  $\lambda$ -dependent factor  $\xi$ . So, for  $\varphi = \phi = 0$  the particle will have the energy-momentum relation of the lattice-Klein-Gordon equation

$$E/\xi = \sqrt{\mu_Q^2 + K^2}, \quad (41)$$

or

$$E^2 = m_Q^2 + \xi^2 K^2, \quad (42)$$

where  $\xi$  is the rescaling factor, and we write

$$K = 2 \sin(P/2), \quad m_Q = \mu_Q \xi. \quad (43)$$

The correct conformal normalization factor  $\xi$  for the  $\mathcal{WA}_{n-1}$ -quantum chains at the critical point  $\lambda = 1$  is well-known[27, 34]:

$$\xi(\lambda = 1) = n. \quad (44)$$

Using formulae (39) and (21), (22), the  $m_Q$  and the rescaling factors for the  $Q = 1$ - and  $Q = 2$ -particles of the  $\mathcal{WA}_{n-1}$ -chains near  $\lambda = 0$  can be calculated explicitly. The  $m_Q$  for  $Q = 1, 2$  have been given in (21), (22) and (23), from which we find:

$$\Delta E_{1,0} = 2 \cot\left(\frac{\pi}{2n}\right) - \frac{2\lambda}{\sin(\pi/n)}(1 - K^2/2) + \dots \quad (45)$$

$$\Delta E_{2,0} = 2 \cot\left(\frac{\pi}{2n}\right) + 2 \cot\left(\frac{3\pi}{2n}\right) - \frac{2\lambda}{\sin(2\pi/n)}(1 - K^2/2) + \dots \quad (46)$$

from which we get different rescaling factors for particles with different charge: Defining

$$\zeta = n\sqrt{\lambda} \quad (47)$$

(coinciding for  $\lambda = 1$  with (44)), for small  $\lambda$  we obtain:

$$\xi_{Q=1}(\lambda) = \frac{\sqrt{2}}{n \sin(\frac{\pi}{2n})} \zeta + \dots \quad (48)$$

and

$$\xi_{Q=2}(\lambda) = \frac{\xi_{Q=1}(\lambda)}{\sqrt{2 \cos^2(\frac{\pi}{2n}) - \frac{1}{2}}} + \dots \quad (49)$$

Putting numbers, we find that the main variation of the  $\xi_Q$  over the whole range  $0 \leq \lambda < 1$  is determined (for low values of  $n$ ) up to 10...20% by the factor  $\zeta$ . E.g. for  $\mathbb{Z}_4$  at  $\lambda \rightarrow 0$  we have

$$\lim_{\lambda \rightarrow 0} \xi_{Q=1}/\zeta = 0.92388\dots \quad \lim_{\lambda \rightarrow 0} \xi_{Q=2}/\zeta = 0.84090\dots \quad (50)$$

similarly for higher  $n$ . For the Ising case  $n = 2$  we have exactly  $\xi_{Q=1} = \zeta$  for all  $\lambda$  [47].

For  $\varphi = \phi = 0$  the two parameters  $\xi$  and  $m_Q$  determine the dispersion curve exactly. E.g. in the  $\mathcal{WA}_2$ -case ( $n = 3$ ) we find for  $\lambda = 0.00, 0.25, 0.50, 0.75, 0.90$ :

$$m_Q/(1 - \lambda)^{5/6} = 3.46410162, 3.58582824(1), 3.674214(2), 3.73(3), 3.8(1) \quad (51)$$

and

$$\xi/\zeta = 0.9428090, 0.9751702(1), 0.996697(2), 1.008(6), 1.00(1), \quad (52)$$

respectively. At  $\lambda = 0.75$  and  $\lambda = 0.9$  we observe a non-monotonous behaviour of the levels with  $N$  which gives rise to a considerable uncertainty in the extrapolation  $N \rightarrow \infty$ . At lower values of  $\lambda$  the exponential convergence clearly sets in already below  $N = 12$  sites, so that there we may trust the extrapolation.

For  $\lambda \rightarrow 0$  the masses determining the  $N$ -convergence go to infinity. So for  $\lambda = 0$  there is no  $N$ -dependence, once a minimal value of  $N$ , dictated by the nearest neighbour-interaction, is reached. This is in agreement with (48) and (49) and shows that the high-temperature expansion around  $\lambda = 0$  at the same time is also a nonrelativistic expansion of (41). For the  $\mathcal{WA}_2$ -case we have checked that the order  $\lambda^2$ -term of (45) agrees with the second order expansion term of (41): We find

$$\Delta E_{1,0} = \frac{2}{\sqrt{3}} \left( 3 - \lambda(2 - K^2) - \lambda^2(1 - K^2 + K^4/6) + \dots \right) \quad (53)$$

which fits to the form

$$\Delta E_{1,0} = m_1 + (\xi K)^2/(2m_1) - (\xi K)^4/(8m_1^3) + \dots \quad (54)$$

So, certainly to this order, the momentum dependence of the  $\mathcal{WA}_2$ -single particle level  $m_1$  is that of the Klein-Gordon equation (41) or (42).

We have no physical interpretation why for low  $n$  the ratio  $\xi_Q/\zeta$  varies so little with  $\lambda$  (in the  $n = 2$ -case we have  $\xi \equiv \zeta$ ), and we find it strange for the particle interpretation that in general,  $\xi_Q(\lambda)$  is  $Q$ -dependent.

For the  $\mathbb{Z}_3$ -superintegrable case Albertini *et al.* [22] have given analytic formulae and plots of the energy-momentum dependence of the  $m_1$ -particle in the high-temperature range  $0 \leq \lambda < 1$ , and for the first  $Q=0$ -excitation in the low-temperature range  $\lambda > 1$ . Here we want to give simple approximate expressions for the dispersion curves of both  $Q = 1$  and  $Q = 2$ -particles, not only for the superintegrable, but also for the general self-dual  $\mathbb{Z}_3$ -chiral model at  $0 \leq \lambda \leq 1$ .

For  $\varphi, \phi > 0$  we have no simple analytic form of the dispersion equation and so we have performed fits to the curves  $E(P)$  given by

$$E(P) = \sum_{m=0}^3 a_m \cos^m(P - P_m) + \sum_{m=1,3} b_m \sin^m(P - P_m) \quad (55)$$

which come out good up to  $\lambda \approx 0.6$ . Table 8 collects some of these fitted coefficients.

For  $\lambda < 0.5$  the convergence in  $N$  is excellent for all  $p$  if we use up to  $N = 12$  sites. For  $\lambda \leq 0.1$  we can nicely fit the data for the momentum dispersion of the  $Q=1$ -particle just using eq.(39). For larger values of  $\lambda$  inspection of the numerical curves and the fits in Table 8 shows that  $P_m$  is decreasing with increasing  $\lambda$ , and in addition, the curves start being unsymmetrical with respect to  $P = P_m$ . The larger the angle  $\varphi$ , and the larger  $\lambda$  is the more terms in the expansion (55) are needed for a reasonable fit. Figs.3 - 5 show momentum distributions for various values of  $\lambda$  and  $\varphi$  together with our fitted curves. As is seen from Fig. 5, for  $\varphi = 2\pi/3$  and  $\lambda = 0.5$  more terms in the expansion would have been needed. As we approach the incommensurate region, e.g. at  $\varphi = 5\pi/6$ ,  $\lambda = 0.3$ , other levels get below the  $m_1$  level at  $|P| > \pi/2$ , so that the identification of the  $m_1$ -dispersion curve gets difficult. It may be that in this region new particle types will show up.

## 7 Conclusions

We have shown that the low-lying spectrum of the massive high-temperature regime of the self-dual  $\mathbb{Z}_n$ -Potts quantum chain at low chiral parameter values  $\varphi \lesssim 2\pi/3$  can be described in terms of  $n-1$  particles which carry  $\mathbb{Z}_n$ -charges  $Q = 1, \dots, n-1$  (we denote their masses by  $m_Q$ ). This is seen by studying the variation of the single-particle masses from their Köberle-Swieca-values at zero chirality  $\varphi = 0$  up to and above the superintegrable value  $\varphi = \pi/2$ . For low inverse temperatures  $\lambda$  we use a perturbation expansion. For higher  $\lambda$  we concentrate on the special cases  $n = 3$  and  $n = 4$  and diagonalize the hamiltonian numerically.

In the  $\mathbb{Z}_3$ -case the mass ratio  $m_2/m_1$  is shown to rise continuously from  $m_2/m_1 = 1$  at  $\varphi = 0$  to  $m_2/m_1 = 2$  for the superintegrable case  $\varphi = \pi/2$ . In the superintegrable case the  $Q=2$ -particle appears precisely at the  $m_1 + m_1$ -scattering threshold. For  $\varphi \rightarrow \pi$ ,  $m_1$  tends to zero. How far the  $Q=2$ -particle survives for  $\varphi > \pi/2$  is not clear. In Table 5 we give evidence that the  $Q = 2$ -single particle level is still present up to  $\lambda = 0.15$  and  $\varphi = 7\pi/12$ . In the superintegrable case we identify two- and three-particle scattering states through their different power behaviour in the chain size  $N$ . The two single particle levels show

exponential convergence in  $N$ . The perturbation expansion of  $m_2$  is shown to diverge at order  $\lambda^2$  for  $\varphi \rightarrow \pi/2$ .

At small  $\lambda$ , the nonconservation of parity in the model results only in the appearance of a  $Q$ -dependent macroscopic momentum  $P_m = (1 - 2Q/n)\phi$  in the energy-momentum dispersion relations of the particles, which is  $P_m = \pm\phi/3$  in the  $\mathbf{Z}_3$ -case. Our numerical data suggest that the average  $P_m$  decreases with increasing  $\lambda$ , perhaps  $P_m \rightarrow 0$  for  $\lambda \rightarrow 1$ , but we have no simple parametrization of the effects of parity violation at large  $\lambda$  and restrict ourselves to giving trigonometrical fit coefficients.

Using the same methods we have also verified in detail that the high-temperature massive spectrum of the chiral  $\mathbf{Z}_4$ -Potts quantum chain can be described analogously in terms of three massive particles with  $\mathbf{Z}_4$ -charges  $Q = 1, 2$  and  $3$ . In the superintegrable case the mass ratio equals the ratio of the charges, such that now both the  $Q = 2$  and  $Q = 3$  particles appear at scattering thresholds. As before, the scattering states can easily be identified by their power behaviour in the chain length  $N$ , while the single particles show exponential convergence with  $N$ .

It would be interesting to use Lüscher's [48] method to obtain numerical information on the phase-shifts or the  $S$ -matrix from the  $N$ -dependence of the multi-particle states.

## Figures

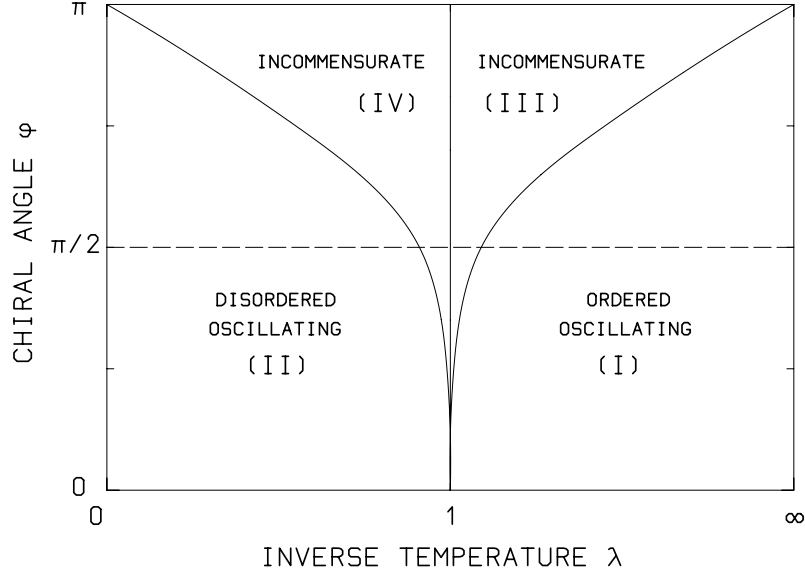


Fig. 1: Schematic phase diagram of the self-dual  $\mathbf{Z}_3$ -chiral Potts-model as defined in eq.(8).

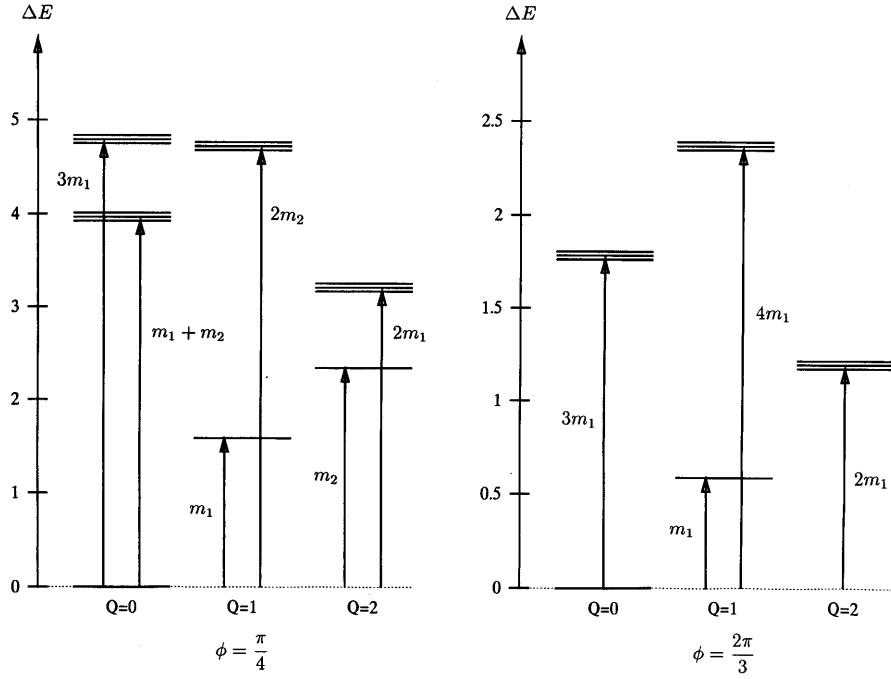


Fig. 2: Level structure for the self-dual  $\mathbb{Z}_3$ -chiral Potts-model in the high-temperature massive region. Left hand side: for a chiral angle  $\varphi < \pi/2$  (below the superintegrable value) and, right hand side:  $\varphi > \pi/2$  (above the superintegrable value). In the latter case the thresholds are determined by  $m_1$  alone.

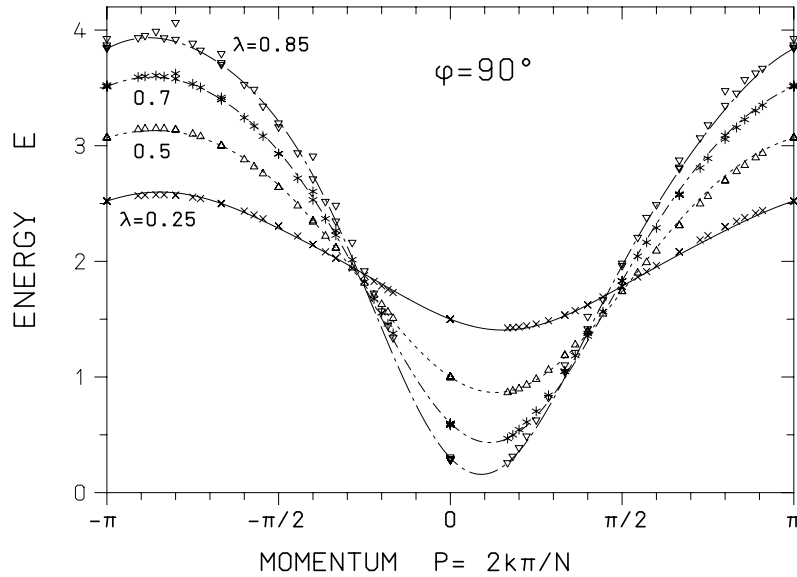


Fig. 3: Energy-momentum relation of particle  $m_1$  for the  $\mathbb{Z}_3$ -superintegrable case and various values of the inverse temperature  $\lambda$  in the high-temperature region. The small crosses and triangles are finite-size values calculated for  $N = 6, \dots, 12$  sites.

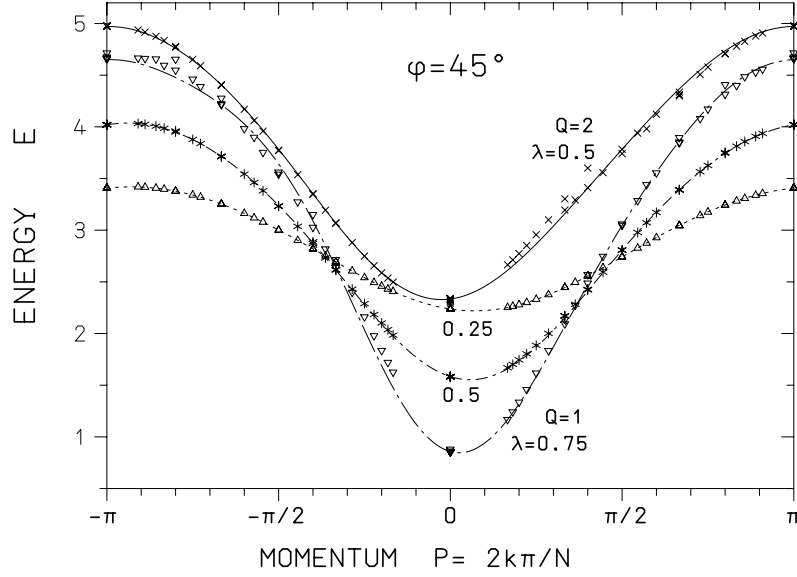


Fig. 4: Same as Fig. 3, but for  $\varphi$  below the superintegrable value and both for  $m_1$  (three dashed curves) and  $m_2$  (full curve).

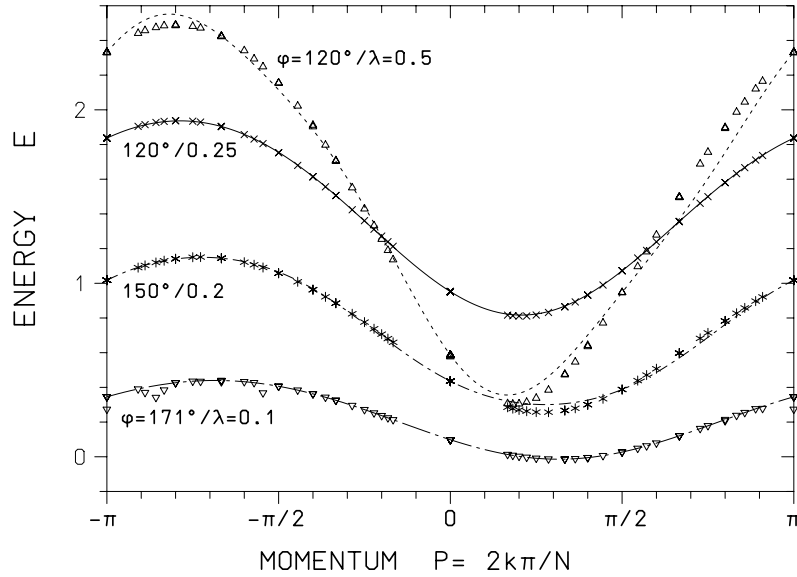


Fig. 5: Same as Fig. 3, but for several values of  $\varphi$  above the superintegrable value (towards the incommensurate region), for the  $Q = 1$ -particle  $m_1$ . The shift of the minima of the curves to the right due to the macroscopic momentum  $P_m$  is clearly seen.

# Tables

$N$	$\Delta E_{Q=0,i}$						
	$i = 1$	2	3	4	5	6	7
7	3.1598983	4.8359585	4.4520381	5.9303676	5.9032240	7.0487030	6.3557797
8	3.1115649	4.4240923	4.2075367	5.4868664	5.5496714	6.3987521	6.0338701
9	3.0808417	4.1213280	4.0168334	5.1252880	5.2384091	5.8572524	5.7243697
10	3.0604137	3.8954662	3.8661605	4.8297326	4.9700825	5.4121174	5.4423701
11	3.0463166	3.7244809	3.7455652	4.5867795	4.7406004	5.0471104	5.1917195
12	3.0362806	3.5932058	3.6478379	4.3856960	4.5446740	4.7471645	4.9714669
$\infty$	2.9998(3)	2.986(7)	3.01(1)	3.02(8)	3.05(6)	2.9(1)	2.95(8)
$y$	3.0(1)	2.9(2)	2.0(1)	2.1(1)	1.9(1)	2.8(6)	?
	$3m_1$	$3m_1$	$m_1 + m_2$	$m_1 + m_2$	$m_1 + m_2$	$3m_1$	?

$N$	$\Delta E_{Q=1,i}$				
	$i = 0$	1	2	3	4
7	0.9984874	4.5173085	5.7905491	6.6049711	6.1612566
8	0.9994289	4.3760023	5.4775432	6.0785242	5.8456347
9	0.9998044	4.2809972	5.2349161	5.6757753	5.5870148
10	0.9999405	4.2150750	5.0442562	5.3652765	5.3749672
11	0.9999851	4.1680556	4.8924532	5.1235743	5.2002368
12	0.9999978	4.1336962	4.7700872	4.9335093	5.0552644
$\infty$	1.0000000	3.99(2)	4.00(1)	4.01(5)	4.01(3)
$y$	expon.	3.0(2)	2.0(1)	2.9(2)	1.9(1)
	$m_1$	$2m_1 + m_2$	$2m_2$	$2m_1 + m_2$	$2m_2$

$N$	$\Delta E_{Q=2,i}$					
	$i = 0$	1	2	3	4	5
7	1.9995726	2.7901373	4.3798245	5.6633417		6.1294869
8	1.9996761	2.6389905	4.0256344	5.3106885	6.0425834	5.8468390
9	1.9998304	2.5261089	3.7351818	4.9697753	5.8323103	5.6487379
10	1.9999247	2.4399607	3.4970152	4.6583108	5.5766919	5.5065400
11	1.9999701	2.3729391	3.3008958	4.3808694	5.3110577	5.4022604
12	1.9999893	2.3198948	3.1384071	4.1365977	5.0527923	5.3242970
$\infty$	2.0001(1)	2.002(7)	2.00(5)	2.0(1)	2.6(5)	4.99(1)
$y$	expon.	2.0(1)	1.9(1)	1.9(2)	?	2.9(2)
	$m_2$	$2m_1$	$2m_1$	$2m_1$	?	$m_1 + 2m_2$

Table 1: The lowest energy gaps  $\Delta E_{Q,i}$ , as defined in eq.(11), for the  $\mathbb{Z}_3$ -hamiltonian eq.(8) and the superintegrable case  $\varphi = \phi = \pi/2$ ,  $\lambda = 0.50$ . The numbers given in brackets indicate the estimated error in the last written digit. All calculations of the gaps have been performed to 12 digit accuracy and using all  $N = 2, \dots, 12$  sites for the extrapolation  $N \rightarrow \infty$ . In order to save space, in the Tables we give less digits and omit the low- $N$ -data. Details on our determination of the exponent of convergence  $y$ , defined in (29), (30) is given in Table 2 below. In the last line of each Table above, we give our particle interpretation of the various levels, as deduced from the result for  $y$ .

$N$	$y_N$ for $\Delta E_{Q=0,i}$				$y_N$ for $\Delta E_{Q=1,i}$			$y_N$ for $\Delta E_{Q=2,i}$		
	$i = 1$	2	3	4	$i = 0$	1	2	$i = 0$	1	2
7	2.6413	1.7475	1.2814	1.0998	5.6670	2.1812	1.3354		1.5124	1.0720
8	2.6955	1.9024	1.3808	1.2290	7.2946	2.3893	1.4389	2.0775	1.5900	1.2068
9	2.7348	2.0293	1.4594	1.3340	9.0948	2.4728	1.5230	5.4923	1.6503	1.3140
10	2.7646	2.1348	1.5222	1.4212	11.2974	2.5376	1.5917	7.7025	1.6973	1.4013
11	2.7879	2.2232	1.5731	1.4947	14.5079	2.5883	1.6482	9.6994	1.7340	1.4733
12	2.8067	2.2976	1.6148	1.5573	21.8070	2.6287	1.6948	11.7909	1.7633	1.5334
$\infty$	3.0(1)	2.9(2)	2.0(1)	2.1(1)	expon.	3.0(2)	2.0(1)	expon.	2.0(1)	1.9(1)

Table 2: Exponents  $y_N$  of the convergence  $N \rightarrow \infty$  as defined in eq.(30), for the  $\mathbf{Z}_3$ -superintegrable case and  $\lambda = 0.5$  for the lower levels given in Table 1. "expon." means that the fast increasing sequence of the  $y_N$  indicates exponential convergence.

$\phi = \varphi = \pi/4, \lambda = 0.5$				$\phi = \varphi = 2\pi/3, \lambda = 0.5$			
$Q$	$i$	$\Delta E_{Q,i}(\infty)$	Particles	$Q$	$i$	$\Delta E_{Q,i}(\infty)$	Particles
0	1	3.9150(2)	$m_1 + m_2$	0	1	1.75(1)	$3m_1$
0	2	3.85(3)	$m_1 + m_2$	0	2	1.80(5)	$3m_1$
0	3	3.98(4)	$m_1 + m_2$	0	3	1.8(1)	$3m_1$
0	4	4.70(8)	$3m_1$	1	0	0.5868(2)	$\equiv m_1$
0	5	3.90(5)	$m_1 + m_2$	1	1	2.36(4)	$4m_1$
1	0	1.5834366(1)	$\equiv m_1$	2	0	1.174(2)	$2m_1$
1	1	4.68(1)	$2m_2$	2	1	1.18(2)	$2m_1$
2	0	2.339607(1)	$\equiv m_2$	2	2	1.19(5)	$2m_1$
2	1	3.168(4)	$2m_1$				
2	2	3.17(5)	$2m_1$				

Table 3: The lowest energy gaps  $\Delta E_{Q,i}$  (extrapolated  $N \rightarrow \infty$ ) of the self-dual  $\mathbf{Z}_3$ -model (8), for  $\lambda = 0.5$  and two values of  $\varphi$ :  $\varphi = \pi/4$  (below the superintegrable line), and  $\varphi = 3\pi/2$  (above the superintegrable line), together with their particle interpretation.

$N$	$\Delta E_{Q=2,i} (\varphi = 7\pi/12, \lambda = 0.10)$ $m_1 = 1.50335845$				$\Delta E_{Q=2,i} (\varphi = 7\pi/12, \lambda = 0.15)$ $m_1 = 1.41131611$			
	$i = 0$	5	6	7	$i = 0$	5	6	7
7	3.03919	3.58623	3.89205	7.99416	2.86777	3.63650	3.95076	7.69924
8	3.03222	3.72696	3.89348	7.90458	2.85847	3.85581	3.98085	7.57893
9	3.02727	3.65640	3.89285	7.83788	2.85177	3.75262	3.96189	7.49035
10	3.02363	3.74332	3.89313	7.78699	2.84678	3.89547	3.97910	7.42310
11	3.02088	3.69394	3.89301	7.74732	2.84297	3.81857	3.96735	7.37073
12	3.01875	3.75171	3.89306	7.71579	2.83999	3.91801	3.97795	7.32905

Table 4: Selected  $Q = 2$ -gaps for  $\varphi = 7\pi/12$  (slightly above the superintegrable line) of the self-dual  $\mathbf{Z}_3$ -model. The numbering of the levels ( $i = 0, \dots$ ) refers to  $N = 12$  sites, for a smaller number of sites there are less levels between  $i = 0$  and  $i = 5$ . The values of  $m_1$  are very well determined because of fast convergence. Observe that the  $i = 0$ -levels converge excellently to  $2m_1$ . In both cases level  $i = 6$  converges much faster with  $N$  than the other levels, which may indicate that this is the  $m_2$ -level. Non-monotonous behaviour in  $N$  is common in the neighbourhood of the IC-phase.

$\varphi = \pi/4, \phi = 19.47\dots^\circ$ $\lambda = 0.75$				$\varphi = 2\pi/3, \phi = 135.58\dots^\circ$ $\lambda = 0.70$			
$Q$	$i$	$\Delta E_{Q,i}(\infty)$	Particles	$Q$	$i$	$\Delta E_{Q,i}(\infty)$	Particles
0	1	1.933(2)	$m_1 + m_2$	0	1	1.50(1)	$3m_1$
0	2	1.9(2)	$m_1 + m_2$	0	2	1.53(5)	$3m_1$
0	3	1.8(3)	$m_1 + m_2$	1	0	0.495(2)	$\equiv m_1$
1	0	0.750(1)	$\equiv m_1$	1	1	1.99(1)	$4m_1$
1	1	2.41(2)	$2m_2$	2	0	0.995(1)	$2m_1$
2	0	1.19(2)	$\equiv m_2$	2	1	1.00(1)	$2m_1$
2	1	1.50(3)	$2m_1$	2	2	1.04(5)	$2m_1$
				2	3	2.52(5)	$5m_1$

Table 5: Lowest energy gaps  $\Delta E_{Q,i}$  as in Table 3, but for two different choices of the parameters in the *integrable*  $\mathbf{Z}_3$ -model case, in which  $\varphi$  and  $\phi$  are related by (7). On the left side we give an example with chiral angles below the superintegrable case, on the right hand side  $\phi, \varphi$  are taken above their superintegrable values. The pattern observed here is very similar to that of the self-dual case in Table 3.

$N$	$\Delta E_{Q=0,i}$				$\Delta E_{Q=1,i}$		
	$i = 1$	2	3	4	$i = 0$	1	2
4	4.4870349	6.6401198	6.9386000	7.1202527	0.9782260	6.2907501	8.8182343
5	4.2443835	6.2079844	6.3448347	6.4390786	0.9932173	5.7339386	7.9355672
6	4.1352996	5.6907770	5.9280172	6.0208759	0.9985794	5.4429212	7.2245463
7	4.0807817	5.3191415	5.5469396	5.7278875	0.9999564	5.2809826	6.8098311
8	4.0511625	5.0477033	5.2606178	5.2880905	1.0001440	5.1860132	6.4550409
9	4.0339657	4.8460464	4.9582447	5.0427288	1.0000927	5.1277432	6.1875836
10	4.0234306	4.6936534	4.7248803	4.8744672	1.0000390	5.0905398	5.9834045
$\infty$	4.0000(2)	3.89(2)	3.9(9)	3.7(4)	1.0001(1)	4.97(3)	5.7(6)
$y$	4.0(2)	2.1(3)	2.9(4)	1.6(1)	expon.	3.5(3)	1.8(1)
	$4m_1$	$2m_2$ or $m_1 + m_3$	$2m_1 + m_2$	$2m_2$ or $m_1 + m_3$	$m_1$	?	$m_2 + m_3$

$N$	$\Delta E_{Q=2,i}$		$\Delta E_{Q=3,i}$		
	$i = 0$	1	$i = 0$	1	2
4	1.9760981	3.6344881	3.0090309	5.0706873	5.4135243
5	1.9885583	3.1951141	2.9978592	4.4899244	4.9297443
6	1.9959972	2.9027708	2.9980224	4.1048393	4.5520862
7	1.9989351	2.7013088	2.9991277	3.8412387	4.2636142
8	1.9998278	2.5582804	2.9997209	3.6558602	4.0432463
9	2.0000213	2.4539476	2.9999379	3.5222475	3.8733462
10	2.0000330	2.3759111	2.9999964	3.4237046	3.7406336
$\infty$	2.00001(3)	1.9(1)	3.00001(6)	2.8(2)	3.02(4)
$y$	expon.	1.9(1)	expon.	2.1(2)	1.7(2)
	$m_2$	$2m_1$	$m_3$	$m_1 + m_2$	$m_1 + m_2$

Table 6: The lowest energy gaps  $\Delta E_{Q,i}$ , as in Table 1, but here instead of the  $\mathbf{Z}_3$ -case now for the  $\mathbf{Z}_4$ -hamiltonian eq.(10). Superintegrable case  $\phi = \varphi = \pi/2$  for  $\lambda = 0.5$ . Note the overshooting in the approximants for  $m_1$  and  $m_2$ .

$\phi = \varphi = \pi/4$ $\lambda = 0.50$			$\phi = \varphi = 3\pi/5$ $\lambda = 0.10$			$\varphi = \pi/4, \phi = 19.47\dots^\circ$ $\lambda = 0.75$					
$Q$	$i$	$\Delta E_{Q,i}(\infty)$	Particles	$Q$	$i$	$\Delta E_{Q,i}(\infty)$	Part.	$Q$	$i$	$\Delta E_{Q,i}(\infty)$	Particles
0	1	5.77(2)	$m_1 + m_3$	0	1	5.1(2)	$4m_1$	0	1	2.767(4)	$m_1 + m_3$
0	2	5.76(8)	$m_1 + m_3$	1	0	1.2116781	$\equiv m_1$	0	2	3.2(1)	$2m_1 + m_2$
0	3	7.1(2)	$2m_2$	1	1	6.1(3)	$5m_1$	1	0	0.8663(1)	$\equiv m_1$
1	0	2.03383(1)	$\equiv m_1$	2	0	2.42334(7)	$2m_1$	1	1	3.50(1)	$2m_1 + m_3$
1	1	7.1958(4)	$m_2 + m_3$	2	1	2.430(6)	$2m_1$	2	0	1.529(2)	$\equiv m_2$
1	2	6.98(7)	$m_2 + m_3$	2	5	3.211450(1)	$\equiv m_2$	2	1	1.8(1)	$2m_1$
2	0	3.4282(1)	$\equiv m_2$	3	0	3.6349(5)	$3m_1$	3	0	1.786(2)	$\equiv m_3$
2	1	4.15(6)	$2m_1$					3	1	2.52(7)	$3m_1$
2	2	4.59(1)	?								
2	3	7.62(7)	$2m_3$								
3	0	3.7501(1)	$\equiv m_3$								
3	1	5.458(2)	$m_1 + m_2$								

Table 7: The left and middle parts of this Table show a selection of lowest energy gaps of the self-dual, but not super-integrable  $\mathbb{Z}_4$ -hamiltonian for two different choices of the parameters  $\phi = \varphi$ , with  $\beta = \tilde{\beta} = 1/\sqrt{2}$  and different  $\lambda$ . The right part of the Table contains an example of the INT case. For most levels in this Table the determination of the convergence exponent  $y$  is very unsafe due to the considerable uncertainty in  $\Delta E_{Q,i}(\infty)$ . So, as also in Tables 3 and 5, the particle content is inferred almost exclusively from  $\Delta E_{Q,i}(\infty)$  alone.

$\varphi$ [deg]	$\lambda$	$a_0$	$a_1$	$a_2$	$a_3$	$b_1$	$b_3$	$\varphi_m$ [deg]
45.	0.25	2.8745	-0.5924	-0.0549	-0.0075	0.0033		39.
45.	0.50	3.0302	-1.1653	-0.2355	-0.0764	-0.0134		30.
45.	0.75	3.3502	-1.6702	-0.6028	-0.2300	0.0864	-0.2121	18.
90.	0.25	2.0436	-0.5118	-0.0412	-0.0848	-0.0112		81.
90.	0.50	2.2363	-1.1331	-0.2381	0.0014	-0.0188		69.
90.	0.70	2.4363	-1.4587	-0.4244	-0.1190	-0.0757	-0.0112	57.
90.	0.85	2.6161	-1.5982	-0.5752	-0.2791	-0.1981	-0.0745	39.
120.	0.25	1.4317	-0.5570	-0.0552	-0.0022	-0.0263		105.
120.	0.50	1.5407	-0.8112	-0.0909	-0.2517	-0.3291		57.
150.	0.20	0.7281	-0.4696	-0.0028	0.0451	0.0013		150.
171.	0.10	0.2257	-0.2260	-0.0128	-0.0009			171.
45.	0.50	3.7927	-1.1973	-0.1501	-0.0874	-0.3223		-45.

Table 8: Coefficients of fits to the energy-momentum relation eq.(55) for various  $\varphi$  and  $\lambda$ , all for the self-dual model. Except for the last line, which is for the lowest  $Q = 2$ -gap, all other fits are for the lowest  $Q = 1$ -gaps. The quality of the fits can be judged from Figs. 3, 4 and 5. In the last column we quote  $\varphi_m$ , which we define by  $P_m = \varphi_m/3$ .

## References

- [1] S. Ostlund; Phys. Rev. **B 24** (1981) 398
- [2] D. A. Huse; Phys. Rev. **B 24** (1981) 5180
- [3] see e.g. T. L. Einstein; *Proc. 10th-John Hopkins Workshop*, ed. K. Dietz and V. Rittenberg, World Scientific, Singapore 1987, p.17
- [4] M. den Nijs; in *Phase Transitions and Critical Phenomena*, ed. C. Domb and J. L. Lebowitz, Vol. **12** (1988) 219, Academic Press
- [5] W. Selke; Phys. Reports **170** (1988) 213
- [6] G. v. Gehlen and V. Rittenberg; Nucl. Phys. **B 230** (1984) 455
- [7] H. U. Everts and H. Röder; J. Phys. A: Math. Gen. **22** (1989) 2475
- [8] M. Marcu, A. Regev and V. Rittenberg; J. Math. Phys. **22** (1981) 2740
- [9] P. Centen, V. Rittenberg and M. Marcu; Nucl. Phys. **B 205** (1982) 585
- [10] E. Fradkin and L. Susskind; Phys. Rev. **D 17** (1978) 2637
- [11] J. B. Kogut; Rev. Mod. Phys. **51** (1979) 659
- [12] T. Vescan, V. Rittenberg and G. von Gehlen; J. Phys. A: Math. Gen. **19** (1986) 1957
- [13] S. Howes, L. P. Kadanoff and M. Den Nijs; Nucl. Phys. **B 215** (1983) 169
- [14] G. v. Gehlen and V. Rittenberg; Nucl. Phys. **B 257** [FS14] (1985) 351
- [15] L. Dolan and M. Grady; Phys. Rev. **D 25** (1982) 1587
- [16] For a recent review see: B. M. McCoy; *Special Functions ICM 90, Satellite Conf. Proc.*, ed. M. Kashiwara and T. Miwa, Springer 1991, p. 245
- [17] L. Onsager; Phys. Rev. **65** (1944) 117
- [18] B. Davies; J. Phys. A: Math. Gen. **23** (1990) 2245
- [19] Sh.-Sh. Roan; *Onsager's Algebra, Loop Algebra and Chiral Potts Model*, preprint MPI für Mathematik Bonn, September 1991
- [20] R. J. Baxter; Phys. Lett. **A 133** (1988) 185; J. Stat. Phys. **57** (1989) 1; Phys. Lett. **A 146** (1990) 110; J. Stat. Phys. **52** (1988) 639
- [21] A. B. Zamolodchikov; Int. J. Mod. Phys. **A 4** (1989) 4235
- [22] G. Albertini, B. M. McCoy, J. H. H. Perk; Phys. Lett. **A 135** (1989) 159; Phys. Lett. **A 139** (1989) 204; *Advanced Studies in Pure Math.* **19** (1989) 1
- [23] H. Au-Yang, B. M. McCoy, J. H. H. Perk, Sh. Tang and M. L. Yan; Phys. Lett. **A 123** (1987) 219
- [24] S. Dashmahapatra, R. Kedem, B. M. McCoy; preprint Stony Brook: *Spectrum and completeness of the 3 state superintegrable chiral Potts model*; ITP-SB 92-11

- [25] V. A. Fateev, A. B. Zamolodchikov; Sov. Phys. JETP **62** (1985) 215 (translation of ZhETF **89** (1985) 380)
- [26] F. C. Alcaraz; J.Phys. A: Math. Gen. **19** (1986) L1085; **20** (1987) 2511
- [27] F. C. Alcaraz; J.Phys. A: Math. Gen. **23** (1990) L1105
- [28] F. C. Alcaraz and A. Lima Santos, Nucl. Phys. **B 275** (1986) 436
- [29] V. A. Fateev and S. Lykhanov, Int. J. Mod. Phys. **A 3** (1988) 507
- [30] A. M. Tselvelick; Nucl.Phys. **B 305** (1988) 675
- [31] J. L. Cardy; preprint Cambridge: *Critical exponents of the chiral Potts model from conformal field theory*, UCSBTH-92-37 (1992)
- [32] V.I. S. Dotsenko; Nucl. Phys. **B 235** (1984) 54
- [33] D. Friedan, Z. Qiu and S. Shenker; Phys. Rev. Lett. **52** (1984) 1575
- [34] G. v. Gehlen, V. Rittenberg and H. Ruegg; J. Phys. A: Math. Gen. **19** (1985) 107
- [35] G. v. Gehlen and T. Krallmann; Bonn preprint (*to appear*)
- [36] G. v. Gehlen; preprint Bonn: *Phase diagramm and two-particle structure of the  $\mathbb{Z}_3$ -chiral Potts model*, HE-92-18
- [37] M. Kohmoto, M. den Nijs and L. P. Kadanoff; Phys. Rev. **B 24** (1981) 5229
- [38] M. Baake, G. v. Gehlen, V. Rittenberg; J. Phys. A: Math. Gen. **20** (1987) L479
- [39] P. Pfeuty; Ann. Phys. **57** (1970) 79
- [40] R. Köberle and J. A. Swieca; Phys. Lett. **B 86** (1979) 209
- [41] I. S. Gradstein and I. M. Ryshik, *Tables of Integrals, Series and Products*, New York & London, 1965, eqs. 1.344, 1.351
- [42] M. Henkel and J. Lacki; Phys. Lett. **A 138** (1989) 105
- [43] J. M. Van den Broek and L. W. Schwartz; SIAM J. Math. Anal. **10** (1979) 658
- [44] R. Burlirsch and J. Stoer; Numer. Math. **6** (1964) 413
- [45] M. Henkel and G. Schütz; J. Phys. A: Math. Gen. **21** (1988) 2617
- [46] B. M. McCoy and Sh. Sh. Roan; Phys. Lett. **A 150** (1990) 347
- [47] G. v. Gehlen, J. Phys. A: Math. Gen. **24** (1991) 5371
- [48] Lüscher, M. and U. Wolff; Nucl. Phys. **B 339** (1990) 222;  
M. Lüscher; Commun. Math. Phys. **104** (1986) 177, **105** (1986) 153